Na^+/H^+ exchangers are required for development and function of vertebrate mucociliary epithelia

Dingyuan I. Sun[1,2], Alexia Tasca[3], Maximilian Haas[3], Grober Baltazar[1,4], Richard M. Harland[1], Walter E. Finkbeiner[2], Peter Walentek[1,3,*]

[1] Molecular and Cell Biology Department, Genetics, Genomics and Development Division, University of California, Berkeley, CA, USA

[2] Department of Pathology, University of California, San Francisco, CA, USA

[3] Renal Division, Department of Medicine, University Freiburg Medical Center, Freiburg, Germany

[4] Current address: Children's Medical Research Institute, Westmead, Australia

Keywords:

Slc9a1, Slc9a2, Slc9a3, NHE1, NHE2 NHE3, cilia, airway, Xenopus

Short title:

NHEs in mucociliary epithelia

[*] Correspondence should be sent to:
Dr. Peter Walentek
University Clinic Freiburg
Department of Internal Medicine IV (Nephrology and General Medicine)
and ZBSA – Center for Biological Systems Analysis
Habsburgerstr. 49, 79104 Freiburg, Germany
Telephone: +49-761-203-97206
Email: peter.walentek@medizin.uni-freiburg.de

ORCID: 0000-0002-2332-6068

Supplemental Figure S1: Expression of *slc9a* genes in later *Xenopus* development and knockdown phenotypes in tadpoles

(**A**) *In situ* hybridization on *Xenopus laevis* tadpoles from stages (st.) 38 and 45. *slc9a1* and *2* were expressed in the otic vesicle (ov) and branchial arches (ba) at st. 38 and in the stomach/small intestine (st/smi) at st. 45. At st. 38, *slc9a3* expression was found in the collecting duct of the pronephros (pn) and in the otic vesicle (ov). St. 38 tadpoles are depicted in lateral view, anterior left. St. 45 tadpoles are depicted in lateral and ventral view, anterior to the right, in order to visualize the stomach. (**B**) RT-PCR on cDNAs derived from embryonic stages (st.) 2 – 31. NTC = non-template control (- cDNA). *atp4a* expression is shown for comparison. *odc* expression served as loading control. (**C**) Dorsal views of uninjected control embryos (control) and embryos, which were unilaterally injected (inj.) with *slc9a1, 2* or *3* MOs depicting developmental defects in morphants. The uninjected left side (uninj.) served as internal control. (**D**) slc9a*1*, *2* or *3* MOs as well as control MO (ctrl. MO) were injected at 4pmol individually and combined knockdown was performed by injections of *slc9a1*, *2* and *3*MO at 1.33pmol each in combination. Stage 40 embryos are depicted in lateral view, anterior to the right to visualize the injected side. Combined knockdown induced a much stronger phenotype than each single knockdown, indicating synergistic contribution of those NHEs to cellular homeostasis and development. (n embryos: ctrl.MO = 16; *slc9a1*MO = 20; *slc9a2*MO = 13; *slc9a3*MO = 18; *slc9a1,2,3*MO = 16).

Supplemental Figure S2: Quantification of neural tube defects upon *slc9a* knockdown and MCC phenotype after pharmacological inhibition in *Xenopus*

(**A**) Quantification of neural tube closure defects depicted in Figure 3A. Normal = phenotype as depicted in control embryo; mild defects = phenotype as depicted in *slc9a3* morphant embryo; severe defects = phenotypes as depicted in *slc9a1* morphant embryo. *** = *P<0.001*, chi-squared test. (**B**) Incidence of white extruded cells around the anterior neural tube, likely representing dead cells in morphants quantified for neural tube closure defects in A. (**C**) Embryos were treated with either DMSO (control) or 200μM EIPA from stage 8/9 to stage 29. Embryos were fixed and stained for MCC cilia (Ac.-α-Tub., blue), F-actin (green) and mucus-like compounds using PNA (Mucins, magenta). In contrast to control-treated embryos (n embryos = 9; n cells = 27), which showed normal ciliation (100%), actin cap formation (100%) and mucus production (97%), analysis of EIPA treated embryos (n embryos = 9; n cells = 27) revealed ciliation defects in 48%, apical actin cap formation defects in 63%, and reduced mucin production in 19% of analyzed cells.

Supplemental Figure S3: Quantification of manipulated MCCs and ISCs upon *slc9a* knockdown

(**A**) The same sets of embryos as depicted in Figure 3A and B were analyzed for presence of MCCs and ISCs in controls and manipulated embryos. Embryos were injected with *clamp-rfp* (red) mRNAs and indicated MOs. Immunofluorescence staining against acetylated-α-tubulin (Ac.-α-Tub., blue) revealed cilia and phalloidin stained the actin cytoskeleton (green). Only RFP-positive (= manipulated) cells were quantified for presence of MCCs and ISCs. MCCs were detected based on acetylated-α-tubulin staining, while ISCs were detected based on their specific morphology (smaller apical surface area and triangular/rectangular shape) as depicted in the

insets. Scale bars indicate magnification. (**B**) Quantification of results revealed no changes in proportions between manipulated MCCs and ISCs in all morphant embryos. Two independent experiments were analyzed (n embryos: ctrl. = 5; *slc9a1*MO = 5; *slc9a2*MO = 5; *slc9a3*MO = 5; *slc9a1,2,3*MO = 5). Number of analyzed cells as indicated in the figure. ns = *P>0.05*, chi-squared test.

Supplemental Movie 1: Loss of NHEs causes reduced fluid flow velocity and defective mucociliary clearance

Representative examples of fluid flow movies are depicted. The movie was reduced in frame rate (1:2) and size. The movie was recorded at 50 frames per second for 10 seconds and plays in real time speed at 25 frames per second (1x).

Sun et al. - Fig. S 1

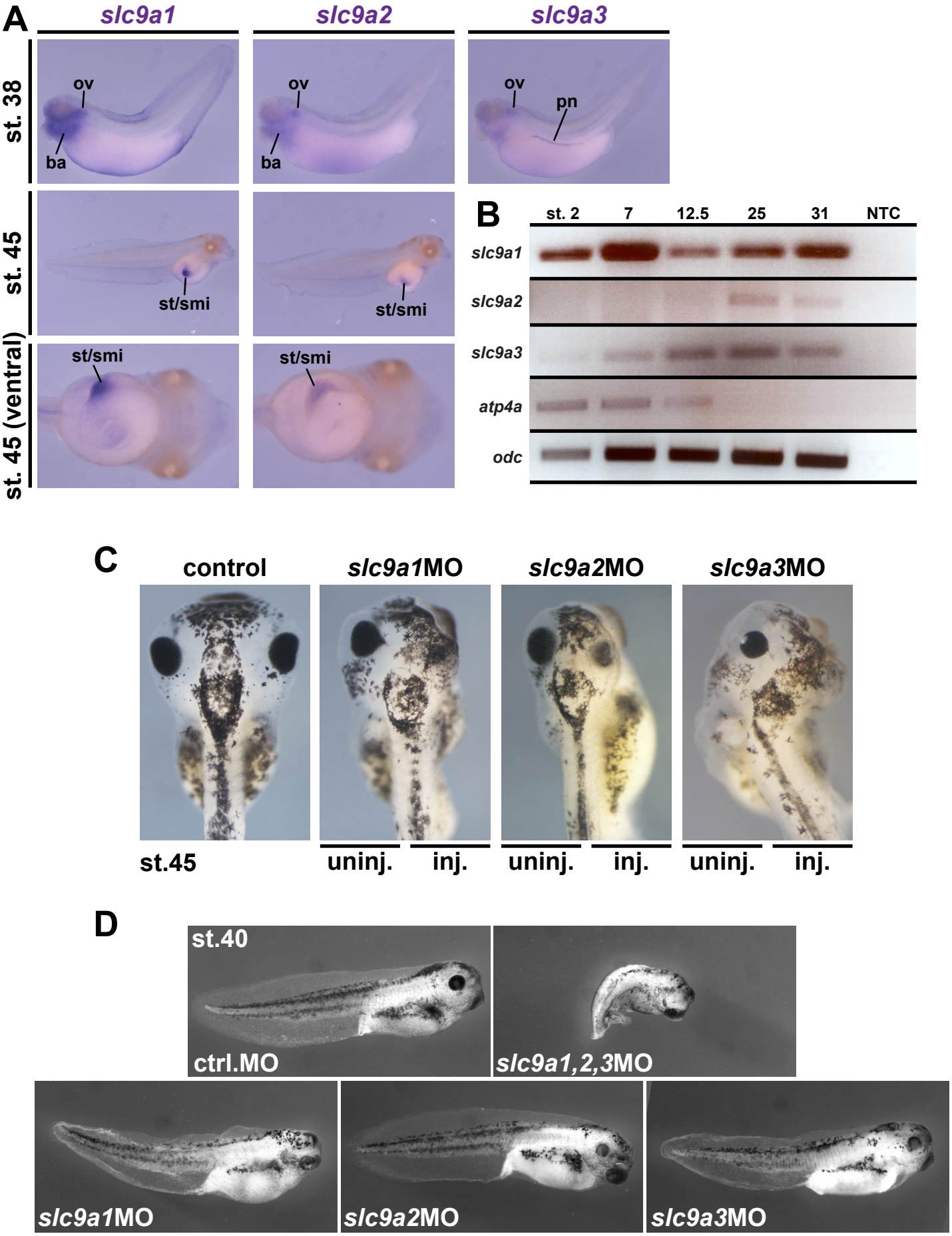

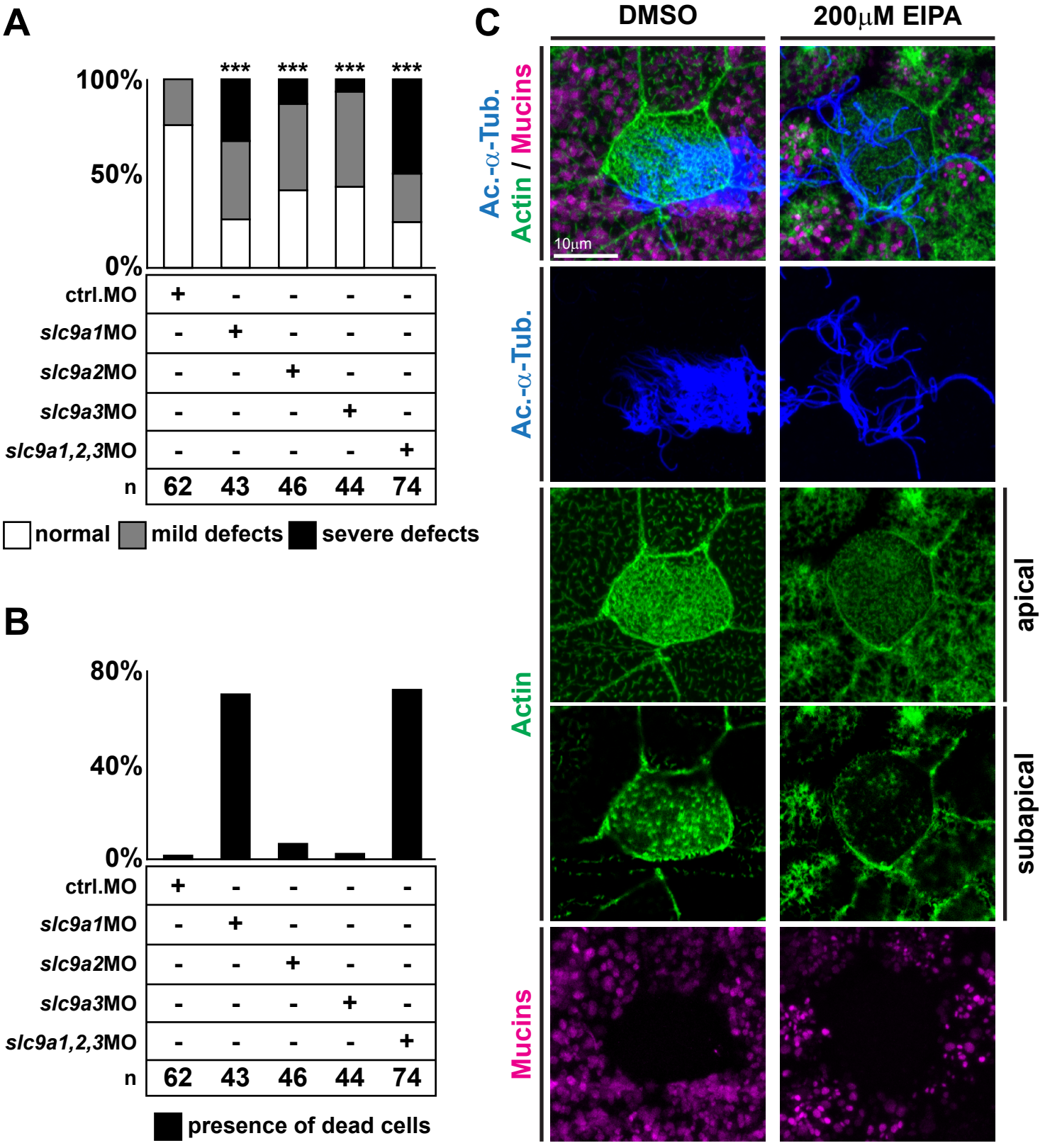
A
100%
50%
0%
***
***
***
***
ctrl.MO + - - - -
slc9a1MO - + - - -
slc9a2MO - - + - -
slc9a3MO - - - + -
slc9a1,2,3MO - - - - +
n 62 43 46 44 74
normal
mild defects
severe defects
B
80%
40%
0%
ctrl.MO + - - - -
slc9a1MO - + - - -
slc9a2MO - - + - -
slc9a3MO - - - + -
slc9a1,2,3MO - - - - +
n 62 43 46 44 74
presence of dead cells
C
DMSO
200μM EIPA
Ac.-α-Tub. Actin / Mucins
10μm
Ac.-α-Tub.
Actin
apical
subapical
Mucins

Sun et al. - Fig. S 3